Mol Biol Rep (2011) 38:2445–2453
DOI 10.1007/s11033-010-0380-z

Studies on the interaction between benzophenone and bovine serum albumin by spectroscopic methods

Ye-Zhong Zhang · Jing Zhang · Fang-Fang Li · Xun Xiang · A-Qiong Ren · Yi Liu

Received: 1 February 2010 / Accepted: 8 November 2010 / Published online: 19 November 2010

Abstract The interaction between benzophenone (BP) and bovine serum albumin (BSA) was investigated by the methods of fluorescence spectroscopy combined with UV–Vis absorption and circular dichroism (CD) measurements under simulative physiological conditions. The experiment results showed that the fluorescence quenching of BSA by BP was resulted from the formation of a BP–BSA complex and the corresponding association constants (K_a) between BP and BSA at four different temperatures had been determined using the modified Stern–Volmer equation. The enthalpy change (ΔH) and entropy change (ΔS) were calculated to be –43.73 kJ mol^{-1} and −53.05 J mol^{-1} K^{-1}, respectively, which suggested that hydrogen bond and van der Waals force played major roles in stabilizing the BP–BSA complex. Site marker competitive experiments indicated that the binding of BP to BSA primarily took place in site I (sub-domain IIA). The conformational investigation showed that the presence of BP decreased the α-helical content of BSA and induced the slight unfolding of the polypeptides of protein, which confirmed some micro-environmental and conformational changes of BSA molecules.

Y.-Z. Zhang (✉) · J. Zhang · F.-F. Li · X. Xiang · A.-Q. Ren · Y. Liu (✉)
Department of Chemistry, College of Chemistry and Environmental Engineering, Yangtze University, Jingzhou 434023, Hubei, People's Republic of China
e-mail: zhangfluorescence@126.com

Y. Liu
e-mail: prof.liuyi@263.net

Y. Liu
State Key Laboratory of Virology, College of Chemistry and Molecular Sciences, Wuhan University, Wuhan 430072, Hubei, People's Republic of China

Keywords Benzophenone · Bovine serum albumin · Fluorescence spectrum · Binding site · Circular dichroism

Introduction

Serum albumin, as the major soluble protein constituents of the circulatory system, is responsible for the maintenance of blood pH and the contribution of colloid osmotic blood pressure. It also plays an important role in the transport and disposition of endogenous and exogenous ligands present in blood. Distribution and metabolism of biologically active compounds such as metabolites, drugs and other organic compounds in the body are correlated with their affinities towards serum albumin [1–4]. Strong binding can decrease the concentrations of free drugs in plasma, whereas weak binding can lead to a short lifetime or poor distribution. Consequently, the investigation of the binding between drugs and serum albumin is of great importance in pharmacology and pharmacodynamics. In this work, bovine serum albumin (BSA) was selected as the protein model because of its availability, low cost, stability, unusual ligand binding properties, and the high homology with human serum albumin (HSA) [5]. On the basis of the distribution of the disulfide bridges and of the amino acid sequence, it seems that BSA is composed of three homologous domains linked together (I–III), and each domain is subdivided into two subdomains (A, B). It has two tryptophan residues that possess intrinsic fluorescence: Trp-134, which is located on the surface of sub-domain IB, and Trp-212, locating within the hydrophobic binding pocket of sub-domain IIA [6]. By monitoring the intrinsic fluorescence change of BSA, information about the distribution, metabolism, and elimination of drugs in vivo and its pharmacological effect on SA can be obtained [7–10].

Benzophenone (BP, C_6H_5-CO-C_6H_5), an aromatic ketone (diphenyl ketone), is a well-known, important intermediate in the preparation of many commercial and industrial materials, such as cosmetics and medicines. It is reported that BP has been used as an ingredient of pharmaceuticals, insecticides, agricultural chemicals and fragrances in medicine industry for more than 30 years. Ongoing research and clinical trials provide ample evidence that benzophenone-compounds possess diverse pharmacological potencies. Besides their effective anti-inflammatory, antimalarial, antianaphylactic, antitubercular, antiviral, antiandrogenic, antimitotic, anti-cancer properties in vitro and in vivo[11–19], these compounds are also considered as inhibitors of HIV, farnesyltransferase and reverse transcriptase and as other pharmaceuticals [20–22].

Most drugs and some bioactive small molecules can extensively and reversibly bind to serum albumin and they are transported mainly as complexes in vivo. As a potential valuable drug, BP can bind to the albumin in blood and then be transported to the target. The nature and magnitude of drug–protein interaction influence the biological activity (efficacy and rate of delivery) of the drug. Thus, it is important to study the interaction between BP and SA for knowing and controlling the pharmacological response of BP. This kind of studies may provide important information on the structural features that determine the therapeutic effectiveness of drugs, and has become an important research field in chemistry, life science and clinical medicine accordingly [4–6]. In this paper, the interaction between BP and BSA was studied under physiological conditions by fluorescence spectroscopy combined with UV–Vis absorption and circular dichroism (CD) spectra. Great attempts were made to investigate the interaction mechanism between BP and BSA regarding the quenching mechanism, the specific binding site, the type of interaction force, and the effect of BP on the micro-environmental and conformational changes of BSA molecules.

Experimental

Materials

BSA (free of fatty acid) was purchased from sigma–Aldrich (St. Louis, MO, USA). The purity of BSA was 98% and free from aggregates. The BSA working solutions with a concentration of 2.0×10^{-6} mol L^{-1} were prepared by dissolving BSA in the Tris–HCl buffer solution (0.10 mol L^{-1} Tris base, 0.10 mol L^{-1} HCl and 0.10 mol L^{-1} NaCl, pH 7.40) and stored in dark prior to use. BP was purchased from Sinopharm Chemical Reagent Co., Ltd (Shanghai, China). The stock solution of BP was prepared by dissolving it in absolute ethanol with the final concentration of 1.0×10^{-3} mol L^{-1}. All other reagents and solvents were of analytical purity and doubly distilled water was used throughout the experiment. The weight measurements were performed on an AY–120 electronic analytic weighting scale (Shimadzu, Japan) with a resolution of 0.1 mg.

Equipment and methods

All fluorescence measurements were performed on an LS–55 Spectrofluorimeter (Perkin–Elmer corporate, America) that equipped with a 1.0 cm quartz cell and a thermostat bath. Fluorescence emission spectra were recorded at four different temperatures (292, 298, 304 and 310 K) in the range of 300–450 nm. The width of the excitation and emission slits was set to 15.0 nm and 4.0 nm, respectively. An excitation wavelength of 285 nm was chosen and the temperature of sample was kept by recycle water during the experiment. All titrations were done manually by trace syringes.

UV–Vis absorption spectrum was recorded on a TU–1901 spectrophotometer (Puxi Analytic Instrument Ltd. of Beijing, China) equipped with 1.0 cm quartz cells. The recorded wavelength was ranging from 500 to 200 nm.

Site marker competitive experiments: binding studies between BP and BSA in the presence of two site markers (warfarin and ibuprofen) were measured using the fluorescence titration methods in two ways. One way is by holding the concentration of BSA equal to that of the site markers, BP was then gradually added to the BSA-warfarin or BSA-ibuprofen mixtures. An excitation wavelength of 285 nm was selected and the fluorescence spectra were recorded in the range of 300–450 nm. The other way is by adding BP gradually to the BSA-warfarin mixture with the excitation wavelength set at 320 nm (the maximum absorption wavelength of warfarin) and the fluorescence spectra was recorded in the range of 340–480 nm.

Circular dichroism (CD) measurements were performed on a J-810 Spectropolarimeter (Jasco, Tokyo, Japan) (pH = 7.4). The CD measurements of BSA in the absence and presence of BP (1:0, 1:2, 1:6, and 1:12) were recorded in the range of 260–200 nm. The instrument was controlled by Jasco's Spectra Manage software. Quartz cells having path length of 0.1 cm were used and a scanning speed of 200 nm min^{-1} was selected. The data were expressed in terms of mean residue ellipticity (MRE). Appropriate buffer solution running under the same conditions was taken as blank and subtracted from the sample spectra.

The three-dimensional fluorescence spectra were performed under the following conditions: the emission wavelength was recorded from 200 to 500 nm; the initial excitation wavelength was 200 nm with an increment of 5 nm, the number of scanning curves was 31, and the other

scanning parameters were the same as those of the fluorescence quenching spectra.

Results and discussions

Fluorescence quenching mechanism and quenching constant

Fluorescence quenching refers to any process that decreases the fluorescence intensity of a fluorophore. A variety of molecular interactions can result in fluorescence quenching, including excited-state reactions, molecular rearrangements, energy transfer, ground-state complex formation, and collisional quenching [23]. The different mechanisms of quenching are usually classified as either dynamic quenching or static quenching and they can be distinguished by their different dependence on temperature or viscosity, or by lifetime measurements [24]. Higher temperatures can result in faster diffusion and then higher dynamic quenching constants. In contrast, increasing of temperature results in decreased stability of complexes, thus the values of the static quenching constants are expected to be smaller [25].

In the present work, the fluorescence quenching spectra of BSA in the presence of different concentrations of BP at four different temperatures (292, 298, 304, and 310 K) were measured to elucidate the quenching mechanism. The effect of BP on the fluorescence intensity of BSA at 298 K is depicted in Fig. 1. Obviously, BSA has a strong fluorescence emission band at 350 nm when excited at 285 nm, which should mainly due to the fluorescence emission of tryptophan residues; while BP has no fluorescence emission under the same condition (*curve L*). When different

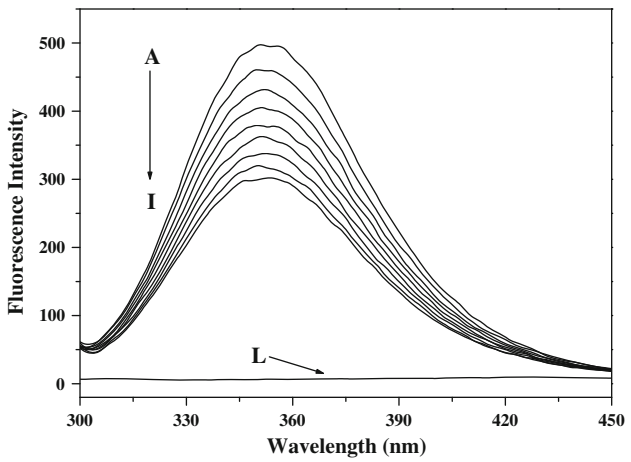

Fig. 1 Emission spectra of BSA in the presence of various concentrations of BP ($T = 298$ K, $\lambda_{ex} = 285$ nm). c(BSA) $= 2.0 \times 10^{-6}$ mol L^{-1}; c(BP)/(10^{-6} mol L^{-1}), A–I: 0, 1.0, 2.0, 3.0, 4.0, 5.0, 6.0, 7.0, 8.0, respectively. *Curve L* shows the emission spectrum of BP only, c(BP) $= 2.0 \times 10^{-6}$ mol L^{-1}

amount of BP was added to a fixed concentration of BSA, a gradually decrease in the fluorescence intensity of BSA was observed, indicating that BP could interact with BSA and quench its intrinsic fluorescence. The fluorescence quenching was usually analyzed using the well-known Stern–Volmer equation [26]:

$$\frac{F_0}{F} = 1 + K_{SV}[Q] = 1 + k_q \tau_0 [Q] \quad (1)$$

where F_0 and F denote the steady-state fluorescence intensities in the absence and presence of quencher (BP), respectively. K_{SV} is the Stern–Volmer quenching constant and $[Q]$ is the concentration of quencher. k_q is the quenching rate constant of the biological macromolecule and k_q is equal to K_{SV}/τ_0. τ_0 is the average lifetime of the molecule without any quencher and the fluorescence lifetime of the biopolymer is 10^{-8}s [27]. The Stern–Volmer plots for the BP–BSA system at four different temperatures are shown in Fig. 2a. Accordingly, Eq. 1 was applied to determine K_{SV} by linear regression of a plot of F_0/F against $[Q]$. The calculated quenching constants K_{SV} and k_q at corresponding temperatures are summarized in Table 1. The results show that K_{SV} is inversely correlated with temperature and k_q is much greater than 2.0×10^{10} L mol^{-1} s^{-1}, which indicate that the fluorescence quenching of BSA was probably induced by the formation of a BP–BSA complex rather than by dynamic collision [28, 29]. In order to confirm the quenching mechanism, the UV–Vis absorption spectra of BSA, BP, and the difference absorption spectra between BSA–BP and BP system were measured at the same concentration (Fig. 3). It reveals that curve *C* (the difference absorption spectra between BP–BSA and BP) was different from curve *B* (the absorption spectra of BSA only), especially in the range of 200–235 nm. This result confirmed that the quenching was mainly a static quenching process [30].

Therefore, the fluorescence quenching of BSA by BP should be analyzed using the modified Stern–Volmer equation [31]:

$$\frac{F_0}{\Delta F} = \frac{F_0}{F_0 - F} = \frac{1}{f_a K_a}\frac{1}{[Q]} + \frac{1}{f_a} \quad (2)$$

In the present case, K_a is the effective quenching constant for the accessible fluorophores, f_a is the fraction of accessible fluorescence. Figure 2b displays the modified Stern–Volmer plots, and the corresponding values of K_a at different temperatures are listed in Table 2. The decreasing trend of K_a with increasing temperature is in accordance with K_{SV}'s dependence on temperature, which coincides with the static quenching mechanism [24]. Besides, the binding constant between BP and BSA is great and the effect of temperature is small, indicating that BP can be stored and carried by protein in the body.

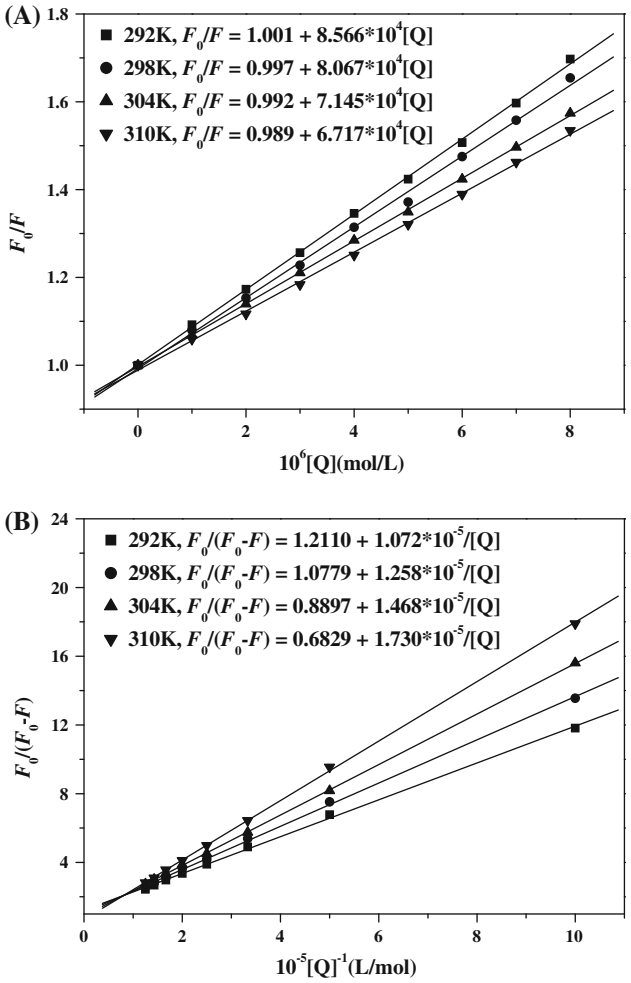

Fig. 2 Stern-Volmer plots (**a**) and modified Stern–Volmer plots (**b**) for the BSA–BP system at four different temperatures, pH 7.4

Table 1 Stern–Volmer quenching constants for the interaction of BP with BSA at four different temperatures

pH	T (K)	K_{SV} ($\times 10^4$ L mol^{-1})	k_q ($\times 10^{12}$ M^{-1} S^{-1})	R^a	SD^b
7.4	292	8.566	8.566	0.9997	0.006
	298	8.067	8.067	0.9987	0.012
	304	7.145	7.145	0.9999	0.003
	310	6.717	6.717	0.9993	0.007

[a] R is the correlation coefficient

[b] SD is the standard deviation for the K_{SV} values

Thermodynamic parameters and type of binding forces

Generally, the interaction forces between small organic molecules and biological macromolecules may include hydrophobic force, hydrogen bond, van der Waals force and electrostatic interactions, etc. [32]. Ross and Subramanian [33] have characterized the signs and magnitudes of the thermodynamic parameters associated with various

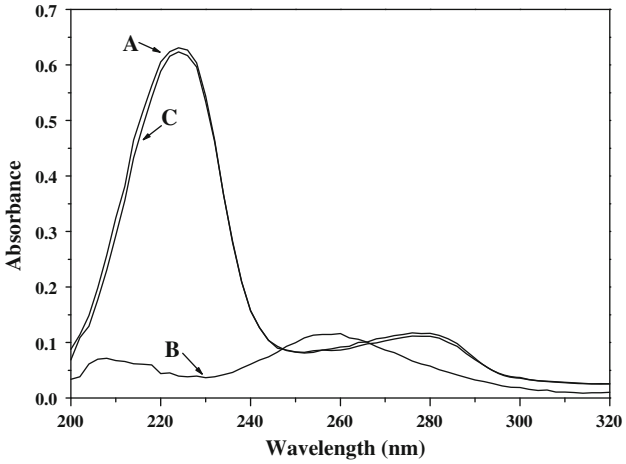

Fig. 3 Effect of BP on UV–Vis spectra of BSA. *A*: The absorption spectrum of BSA only; *B*: The absorption spectrum of BP only; and *C*: The difference absorption spectrum between BP–BSA and BP at the same concentration. c(BP) = c(BSA) = 2.0 × 10^{-6} mol L^{-1}

kinds of interaction force that may take place in protein association process. Considering the dependence of the binding constant (BP–BSA) on temperature, a thermodynamic process was considered to be responsible for the formation of the complex. Thermodynamic parameters for a binding interaction can be used as major evidence for the nature of intermolecular forces [34]. The enthalpy (ΔH) of the reaction of BP and BSA can be treated as a constant in case there is no remarkable change on temperature and the thermodynamic parameters can be calculated from the Van't Hoff equation:

$$\ln K = -\frac{\Delta H}{RT} + \frac{\Delta S}{R} \quad (3)$$

$$\Delta G = \Delta H - T\Delta S = -RT \ln K \quad (4)$$

where K corresponds to the effective binding constant K_a and R is the gas constant. The value of ΔH and ΔS can be calculated from the slope and intercept of the plot of ln$K$ versus $1/T$ (Fig. 4). ΔG value was obtained according to Eq. 4. All the values above were summarized in Table 2. It was observed that the formation of the BSA–BP complex was a spontaneous process with a negative value of ΔG. The values of ΔH (−43.73 kJ mol^{-1}) and ΔS (−53.05 J mol^{-1} K^{-1}) indicate that the hydrogen bond and van der Waals force played a major role in the interaction of BP with BSA [30].

Identification of the binding location of BP on BSA

The three-dimensional structure of crystalline albumin reveals that BSA comprises of three homologous domains (I, II, and III) that assemble to form a heart-shaped molecule [35], each domain contains two subdomains (A and

Table 2 Modified Stern–Volmer association constants K_a and thermodynamic parameters of the BP–BSA system

T (K)	K_a ($\times 10^4$ L mol^{-1})	R^a	ΔH (kJ mol^{-1})	ΔG (kJ mol^{-1})	ΔS (J mol^{-1} K^{-1})	R^b
292	11.29	0.9994	–43.73	–28.24	–53.05	0.9937
298	8.518	0.9996		–28.13		
304	6.060	0.9999		–27.83		
310	3.947	0.9998		–27.27		

[a] R is the correlation coefficient for the K_a values

[b] R is the correlation coefficient for the Van't Hoff plot

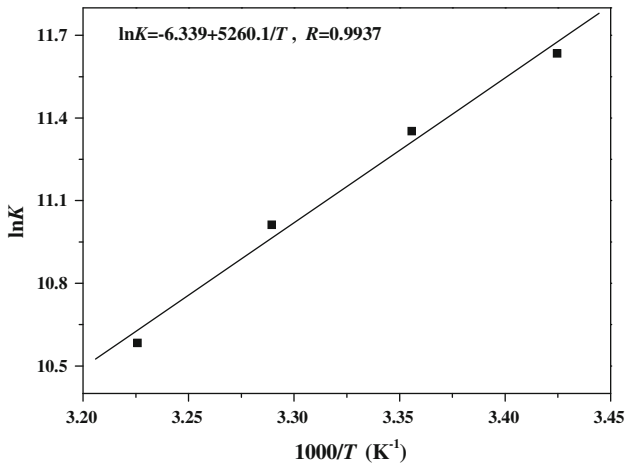

Fig. 4 Van't Hoff plot for the interaction between BSA and BP in Tris–buffer, pH = 7.40

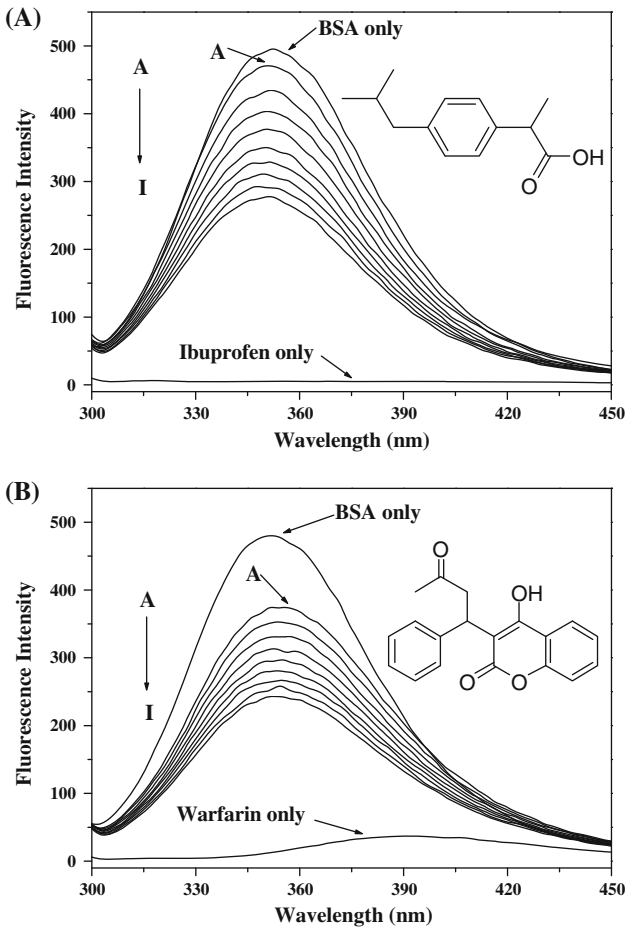

Fig. 5 Effect of selected site markers on the fluorescence of BP bound BSA (T = 298 K, λ_{ex} = 285 nm). **a** c(BSA) = c(Ibuprofen) = 2.0 × 10^{-6} mol L^{-1}; **b** c(BSA) = c(Warfarin) = 2.0 × 10^{-6} mol L^{-1}; c(BP)/(10^{-6}mol L^{-1}), A–I: 0, 1.0, 2.0, 3.0, 4.0, 5.0, 6.0, 7.0, 8.0, respectively. The inserts correspond to the molecular structures of site markers

B). The principal binding regions of drugs to BSA are located in the hydrophobic cavities of subdomains IIA and IIIA, which exhibit similar chemistry properties [17]. The binding cavities associated with sub-domains IIA and IIIA are also referred to as site I and site II according to the terminology proposed by Sudlow et al. [33]. As described in the literature [36], warfarin has been demonstrated to bind at sub-domain IIA, while ibuprofen is considered as sub-domain IIIA binder. In order to identify the binding site of BP on BSA, site marker competitive experiments were carried out in two ways. In the experiments, the drugs warfarin and ibuprofen which specifically bind to known sites or regions on BSA were used. Then information about the binding site can be gained by monitoring the changes in the fluorescence of BP bound BSA that brought about by site I (warfarin) and site II (ibuprofen) markers.

In the first way of site marker competitive experiment, BP was gradually added to the solution of BSA with site markers held in equimolar concentrations (2.0 × 10^{-6} mol L^{-1}). With the addition of ibuprofen into the BSA solution, the fluorescence property of the BP–BSA system was almost the same as that of without ibuprofen (Fig. 5a), which suggested that ibuprofen did not prevent the binding of BP in its usual binding location. By contrast, the addition of warfarin into BSA solution resulted in the slightly red shift of the maximum emission wavelength of BSA and the significantly decrease of the fluorescence intensity (Fig. 5b). Then, with the continuing addition of BP into the above system, the fluorescence intensity of BSA decreased gradually and the intensity was much lower than that of without warfarin. This indicated an increased polarity of the microenvironment surrounding tryptophan (Trp-214) and an obviously affection of the bound BP to BSA by the

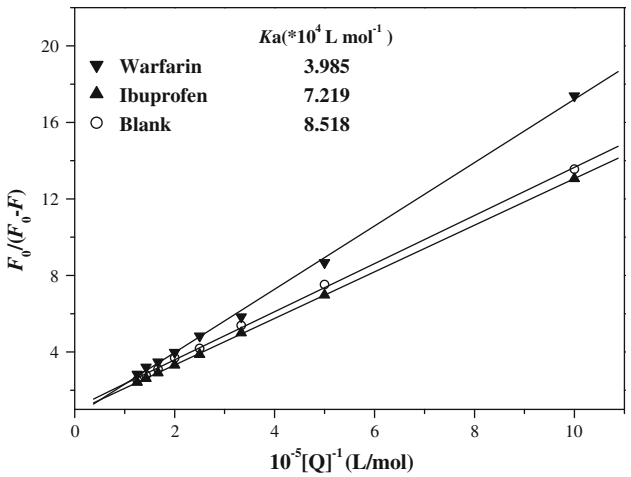

Fig. 6 Modified Stern–Volmer plots for the BP–BSA system in the absence and presence of site markers ($T = 298$ K, pH 7.4)

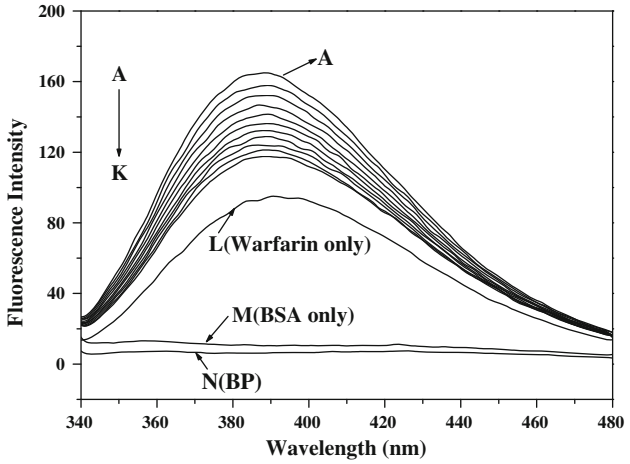

Fig. 7 Displacement of BSA bound warfarin by BP ($T = 298$ K, $\lambda_{ex} = 320$ nm). c(BSA) $= 2.0 \times 10^{-6}$ mol L^{-1}; c(Warfarin) $= 5.0 \times 10^{-6}$ mol L^{-1}; c(BP)/(10^{-5} mol L^{-1}), A–K: 0, 0.2, 0.4, 0.6, 0.8, 1.0, 1.2, 1.4, 1.6, 1.8, 2.0, respectively

adding warfarin. To facilitate the comparison of the influence of warfarin and ibuprofen on the binding of BP to BSA, the binding constants with the presence of site markers were analyzed using the modified Stern–Volmer equation, as shown in Fig. 6. The binding constants of the systems, which can be calculated from the slope values of the plots, were listed in Fig. 6. Obviously, the binding constant of the system with warfarin was almost 46.8% of that without warfarin, while the constants of the systems with and without ibuprofen had only a small difference, indicating that warfarin could significantly affect the binding of BP to BSA, while ibuprofen had only a small influence. The above experimental results and analysis demonstrated that the decrease in BSA fluorescence was resulted from the competitive displacement of the probe, and the binding of BP to BSA mainly located within site I (sub-domain IIA).

In order to verify the above conclusion, another experiment of site marker competitive was carried out by gradually addition of BP into the system of wafarin and BSA. The characteristic emission curves were shown in Fig. 7. It reveals that wafarin has a strong fluorescence peak at 390 nm when excited at 320 nm (*curve L*), while BSA and BP almost have no fluorescence emission when excited at the same wavelength. Moreover, the addition of BSA to the warfarin solution induced a slight blue shift (from 391 nm to 386 nm) of the maximum emission wavelength and a remarkable increase of the fluorescence intensity of warfarin (*curve A*). Then, with the addition of BP to the above warfarin-BSA system, the fluorescence intensity decreased gradually, accompanying with a small extent of red shift of the maximum emission wavelength. It can be expected that with the continued addition of BP, the fluorescence spectrum of the warfarin-BSA system would finally changed to the one similar to *curve L*. The above experimental results suggested that BP had replaced the binding of warfarin to BSA [37], which was consistent with the previous conclusion and confirmed the sub-domain IIA (site I) binding site of BP to BSA.

Conformational investigations

When drugs interacted with BSA, the intramolecular forces that responsible for maintaining the secondary or tertiary structures of protein can be affected, which may further result in a conformational change of protein. To get insight of the structural changes of BSA induced by BP binding, the circular dichroism (CD) and three-dimensional fluorescence spectra of BSA were measured.

CD spectrum has been demonstrated to be a sensitive technique in monitoring the secondary structural change of protein upon interaction with drugs [2]. The CD spectra of BSA exhibits two negative bands at 208 and 222 nm, characteristic of the typical α-helix structure of protein [38]. The reasonable explanation is that the negative peaks of 208–209 nm and 222–223 nm both contribute by the $n \rightarrow \pi^*$ transfer for the peptide bond of α-helixes. The CD spectra of BSA with various concentrations of BP at pH 7.4 and room temperature are shown in Fig. 8. It can be seen that the relative band intensity of *curves A–D* decreased regularly with the increasing addition of BP, suggesting the change of the protein secondary structure. This might be induced by the formation of the BP–BSA complex. The CD curves of BSA in the presence and absence of BP were similar in shape, indicating that the structure of BSA was still predominantly of α-helix. In order to quantify the content of different secondary structure of BSA, the algorithm SELCON3 was applied to analyze the CD spectra,

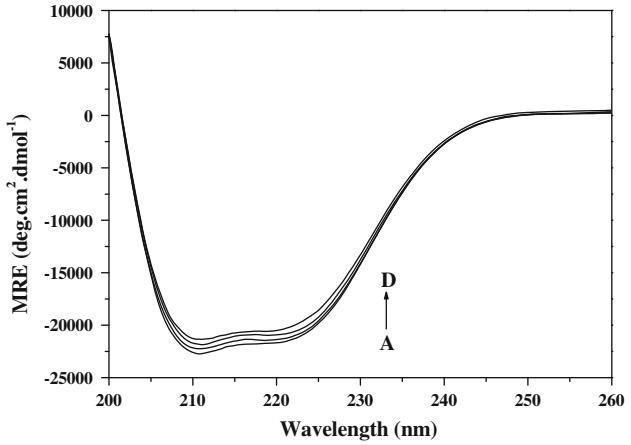

Fig. 8 The CD spectra of the BP–BSA system obtained in Tris–buffer at room temperature and pH 7.4. c(BSA) = 2.0 × 10^{-6} mol L^{-1}; c(BP)/(10^{-6} mol L^{-1}) A–D: 0, 4.0, 12.0, 24.0, respectively

using 43 mode proteins with known precise secondary structures as the reference set [39, 40].

The fraction contents of different secondary structures of BSA in the absence and presence of BP are listed in Table 3. A decreasing tendency of the α-helix content (from 62.5 to 59.2%) and an increasing tendency of β-strands, turn, and unordered structure contents were observed with the increasing concentration of BP. This revealed that the polypeptides of BSA had alternatively unfolded and the secondary structure had been potential perturbation at high drug concentrations. The conformational changes here meant that BP bound with the amino acid residues of the main polypeptide chain of BSA and destroyed their hydrogen bonding networks, making the serum albumin adopt a more incompact conformation state [41].

Three-dimensional fluorescence spectrum (3-D FL), which can comprehensively exhibit the fluorescence information of the chromophore and make the investigation of the characteristic conformational change of protein be more scientific, was applied in the present work. The 3-D FL of BSA and BP–BSA system are shown in Fig. 9, and the corresponding characteristic parameters are listed in Table 4. By comparing the spectral changes of BSA in the

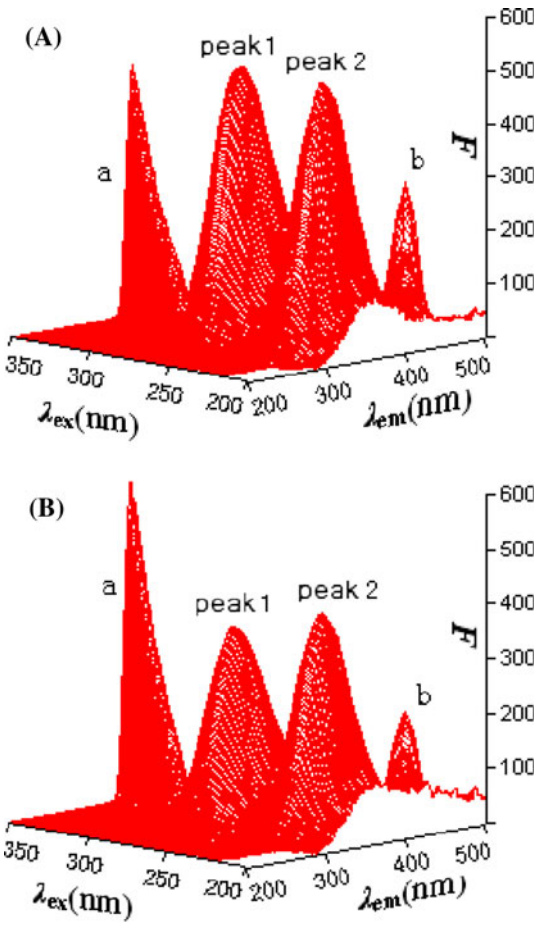

Fig. 9 Three-dimensional fluorescence spectra of BSA (**A**) and BP–BSA system (**B**). c(BSA): (**A**) 2.0 × 10^{-6} mol L^{-1}, (**B**) 2.0 × 10^{-6} mol L^{-1}; c(BP): (**A**) 0, (**B**) 5.0 × 10^{-6} mol L^{-1}

absence and presence of BP, the conformational and micro-environmental changes of BSA can be obtained. As shown in Fig. 9, peak a is the Rayleigh scattering peak ($\lambda_{ex} = \lambda_{em}$), peak b is the second-ordered scattering peak ($\lambda_{em} = 2\lambda_{ex}$) [25], and the fluorescence intensity of peak a increased with the addition of BP. The reasonable explanation is that a BSA–BP complex came into being after the addition of BP, making the diameter of the macromolecule increased, which in turn resulted in the enhancement of the scattering effect [42].

Table 3 Fractions of different secondary structures determined by SELCON3

Molar ratio [BP]:[BSA]	$H(r)$ (%)	$H(d)$ (%)	$S(r)$ (%)	$S(d)$ (%)	Trn (%)	Unrd (%)
0:1	42.5	20.0	2.4	2.6	12.6	19.9
2:1	41.9	19.9	2.6	2.8	12.6	20.2
6:1	40.9	19.8	2.9	2.9	13.0	20.5
12:1	39.6	19.6	3.2	3.2	13.5	20.9

$H(r)$ regular α-helix, $H(d)$ distorted α-helix, $S(r)$ regular β-strand, $S(d)$ distorted β-strand, *Trn* turns, *Unrd* unordered structure

Table 4 Three-dimensional fluorescence spectral characteristic parameters of BSA and BP–BSA system

Peaks	BSA			BP–BSA		
	Peak position	Stokes shift		Peak position	Stokes shift	
	$\lambda_{ex}/\lambda_{em}$ (nm/nm)	$\Delta\lambda$ (nm)	Intensity F	$\lambda_{ex}/\lambda_{em}$ (nm/nm)	$\Delta\lambda$ (nm)	Intensity F
Rayleigh scattering peaks	280/280 → 350/350	0	43.6 → 468.2	280/280 → 350/350	0	46.1 → 580.5
Fluorescence peak 1	280.0/352.0	72.0	502.1	280.0/351.0	71.0	354.1
Fluorescence peak 2	230.0/352.0	122.0	501.3	230.0/351.0	121.0	404.0

Peak 1 ($\lambda_{ex} = 280.0$ nm, $\lambda_{em} = 352.0$ nm) mainly reveals the spectral behavior of tryptophan and tyrosine residues, the maximum emission wavelength and the fluorescence intensity of the residues are in close correlation with the polarity of the microenvironment [43]. Besides peak 1, there is another strong fluorescence peak (peak 2, $\lambda_{ex} = 230.0$ nm, $\lambda_{em} = 352.0$ nm) that mainly exhibits the fluorescence characteristic of polypeptide backbone structures C=O of BSA [2]. As shown in Fig. 9, the fluorescence intensity of peak 2 decreased obviously (from 501.3 to 404.0) after the addition of BP, which indicated that the interaction of BP with BSA induced the unfolding of the polypeptides and conformational change of BSA. Analyzing from the fluorescence intensity changes of peak 1 and peak 2 (the intensity values were listed in Table 4), they both decreased obviously but to different degrees: the fluorescence intensity of peak 1 has been quenched of 29.5% while peak 2 of 19.4%. In combination with the decrease of the fluorescence intensity of the two peaks and the CD experimental results, it can be concluded that the interaction of BP with BSA induced the slight unfolding of the polypeptides of protein, which further resulted in a conformational change of the protein that increased the exposure of some hydrophobic regions which were previously buried [44]. All these phenomenon and analyses of peak 1 and peak 2 revealed that the binding of BP to BSA induced some micro-environmental and conformational changes in BSA.

Conclusions

The present work provided an approach for studying the interaction of BP with BSA by employing spectroscopic methods including fluorescence, UV–Vis absorption, and CD spectroscopy. It demonstrated that the fluorescence quenching of BSA was mainly induced by a static quenching mechanism and hydrogen bond and van der Waals force played major roles in stabilizing the BP–BSA complex. The site marker competitive experiments revealed that the binding site of BP on BSA was located in site I (sub-domain IIA). Results from the CD and 3-D FL investigation demonstrated that the binding of BP to BSA resulted in some extent of conformational and micro-environmental changes of BSA.

Acknowledgments We gratefully acknowledge the financial support of Chinese 863 Program (2007AA06Z407); National Natural Science Foundation of China (Grant Nos. 30570015).

References

1. Colmenarejo G (2003) In silico prediction of drug-binding strengths to human serum albumin. Med Res Rev 23(3):275–301. doi:10.1002/med.10039
2. Zhang YZ, Xiang X, Mei P, Dai J, Zhang LL, Liu Y (2009) Spectroscopic studies on the interaction of Congo Red with bovine serum albumin. Spectrochim Acta A 72:907–914. doi:10.1016/j.saa.2008.12.007
3. Carter DC, Ho JX (1994) Structure of serum albumin. Adv Protein Chem 45:153–203. doi:10.1016/S0065-3233(08)60640-3
4. Zsila F, Bikadi Z, Simonyi M (2003) Probing the binding of the flavonoid, quercetin to human serum albumin by circular dichroism, electronic absorption spectroscopy and molecular modelling methods. Biochem Pharmacol 65:447–456. doi:10.1016/s0006-2952(02)01521-6
5. Tong JQ, Zhang HX, Yang HM, Mei P (2009) Photochemical studies on the binding of an organic fluoride to bovine serum albumin. Mol Biol Rep 37(4):1741–1747. doi:10.1007/s11033-009-9598-z
6. Kragh-Hansen U (1981) Molecular aspects of ligand binding to serum albumin. Pharmacol Rev 33(1):17–53
7. Singh SK, Kishore N (2008) Calorimetric and spectroscopic studies on the interaction of methimazole with bovine serum albumin. J Pharm Sci-US 97:2362–2372. doi:10.1002/jps.21140
8. Wang N, Ye L, Yan FF, Xu R (2008) Spectroscopic studies on the interaction of azelnidipine with bovine serum albumin. Int J Pharm 351:55–60. doi:10.1016/j.ijpharm.2007.09.016
9. Xiao JB, Shi J, Cao H, Wu SD, Ren FL, Xu M (2007) Analysis of binding interaction between puerarin and bovine serum albumin by multi-spectroscopic method. J Pharmaceut Biomed 45:609–615. doi:10.1016/j.jpba.2007.08.032
10. Carnero Ruiz C, Hierrezuelo JM, Peula-Garcı JM, Aguiar J (2007) Physicochemical Studies on the interaction between *N*-decanoyl-*N*-methylglucamide and bovine serum albumin. Biomacromolecules 8:2497–2503. doi:10.1021/bm0704121
11. Chen JJ, Ting CW, Hwang TL, Chen LS (2009) Benzophenone derivatives from the fruits of *Garcinia multiflora* and their anti-inflammatory activity. J Nat Prod 72(2):253–258. doi:10.1021/np8006364
12. Venu TD, Shashikanth S, Khanum SA, Naveen S, Firdouse A, Sridhar MA, Prasadb JS (2007) Synthesis and crystallographic

analysis of benzophenone derivatives—the potential anti-inflammatory agents. Bioorgan Med Chem 15(10):3505–3514. doi:10.1016/j.bmc.2007.02.051
13. Kohring K, Wiesner J, Altenkamper M, Sakowski J, Silber K, Hillebrecht A, Haebel P, Dahse HM, Ortmann R, Priv.-Doz HJ, Klebe G, Schlitzer M (2008) Development of benzophenone-based farnesyltransferase inhibitors as novel antimalarials. Chem Med Chem 3(8):1217–1231. doi:10.1002/cmdc.200800043
14. Neves JS, Coelho LP, Cordeiro RSB, Veloso MP, Silva PMRE, Dos Santos MH, Martins MA (2007) Antianaphylactic properties of 7-epiclusianone, a tetraprenylated benzophenone isolated from *Garcinia brasiliensis*. Planta Med 73(7):644–649. doi:10.1055/s-2007-981534
15. Chen JJ, Ting CW, Chen IS, Peng CF, Huang WT, Su YC, Lin SC (2008) New polyisoprenyl benzophenone derivatives and antitubercular constituents from *Garcinia multiflora*. Planta Med 74(9):1042
16. Ferris RG, Hazen RG, Roberts GB, Clair MHS, Chan JH, Romines KR, Freeman GA, Tidwell JH, Schaller LT, Cowan JR, Short SA, Weaver KL, Selleseth DW, Moniri KR, Boone LR (2005) Antiviral activity of GW678248, a novel benzophenone nonnucleoside reverse transcriptase inhibitor. Antimicrob Agents Ch 203(10):4046–4051. doi:10.1128/AAC.49.10.4046-4051.2005
17. Suzuki T, Kitamura S, Khota R, Sugihara K, Fujimotob N, Ohta S (2005) Estrogenic and antiandrogenic activities of 17 benzophenone derivatives used as UV stabilizers and sunscreens. Toxicol Appl Pharm 203(1):9–17. doi:10.1016/j.taap.2004.07.005
18. Liou JP, Chang CW, Song JS, Yang YN, Yeh CF, Tseng HY, Lo YK, Chang YL, Chang CM, Hsieh HP (2002) Synthesis and structure–activity relationship of 2-aminobenzophenone derivatives as antimitotic agents. J Med Chem 45(12):2556–2662. doi:10.1021/jm010365+
19. Wang Z, Lee HJ, Wang L (2009) Anti-androgen receptor signaling and prostate cancer inhibitory effects of sucrose- and benzophenone-compounds. Pharm Res-Dord 26(5):1140–1148. doi:10.1007/s11095-009-9833-2
20. Fuller RW, Blunt JW, Boswell JL (1999) HIV-inhibitory natural products. 49. Guttiferone F, the first prenylated benzophenone from *Allanblackia stuhlmannii*. J Nat Prod 62(1):130–132. doi:10.1021/np9801514
21. Esteva MI, Kettler K, Maidana C (2005) Benzophenone-based farnesyltransferase inhibitors with high activity against *Trypanosoma cruzi*. J Med Chem 48(23):7186–7191. doi:10.1021/jm050456x
22. Ren J, Chamberlain PP, Stamp A (2008) Structural basis for the improved drug resistance profile of new generation benzophenone non-nucleoside HIV-1 reverse transcriptase inhibitors. J Med Chem 51(16):5000–5008. doi:10.1021/jm8004493
23. Hu YJ, Liu Y, Zhang LX (2005) Studies of interaction between colchicine and bovine serum albumin by fluorescence quenching method. J Mol Struct 750:174–178. doi:10.1016/j.molstruc.2005.04.032
24. Lakowicz JR (2006) Principles of fluorescence spectroscopy, 3rd edn. Springer, New York, pp 277–285
25. Zhang HX, Gao S, Yang XX (2009) Synthesis of an octupolar compound and its biological effects on serum albumin. Mol Biol Rep 36(6):1405–1411. doi:10.1007/s11033-008-9329-x
26. Bose B, Dube A (2006) Interaction of Chlorin p6 with bovine serum albumin and photodynamic oxidation of protein. J Photoch Photobio B 85:49–55. doi:10.1016/j.jphotobiol.2006.04.005
27. Kathiravan A, Renganathan R, Anandan S (2009) Interaction of colloidal AgTiO2 nanoparticles with bovine serum albumin. Polyhedron 28:157–161. doi:10.1016/j.poly.2008.09.023
28. Ware WR (1962) Oxygen quenching of fluorescence in solution, an experimental study of the diffusion process. J Phys Chem 66:455–458
29. Kathiravan A, Chandramohan M, Renganathan R, Sekar S (2009) Spectroscopic studies on the interaction between phycocyanin and bovine serum albumin. J Mol Struct 919:210–214. doi:10.1016/j.molstruc.2008.09.005
30. Zhang YZ, Dai J, Xiang X, Li WW, Liu Y (2009) Studies on the interaction between benzidine and bovine serum albumin by spectroscopic methods. Mol Biol Rep 37(3):1541–1549. doi:10.1007/s11033-009-9555-x
31. Hu YJ, Ou-Yang Y, Dai CM, Liu Y, Xiao XH (2010) Binding of berberine to bovine serum albumin: spectroscopic approach. Mol Biol Rep. doi: 10.1007/s11033-010-0038-x
32. Leckband D (2000) Measuring the forces that control protein interactions. Annu Rev Bioph Biom 29:1–26
33. Ross DP, Subramanian S (1981) Thermodynamics of protein association reactions: forces contributing to stability. Biochemistry-US 20:3096–3102. doi:10.1021/bi00514a017
34. Liu HY, Xu ZH, Liu XH, Xi PX, Zeng ZZ (2009) Analysis of binding interaction between bovine serum albumin and the cobalt(II) complex with salicylaldehyde-2-phenylquinoline-4-carboylhydrazone. Chem Pharm Bull 57(11):1237–1242. doi:10.1248/cpb.57.1237
35. Zhang HX, Huang X, Zhang M (2008) Spectral diagnostics of the interaction between pyridoxine hydrochloride and bovine serum albumin in vitro. Mol Biol Rep 35:699–705. doi:10.1007/s11033-007-9143-x
36. Hu YJ, Ou-Yang Y, Dai CM, Liu Y, Xiao XH (2010) Site-selective binding of human serum albumin by palmatine: spectroscopic approach. Biomacromolecules 11:106–112. doi:10.1021/bm900961e
37. Sahoo BK, Ghosh KS, Dasgupta S (2008) Investigating the binding of curcumin derivatives to bovine serum albumin. Biophys Chem 132:81–88. doi:10.1016/j.bpc.2007.10.007
38. Liu JQ, Tian JN, Tian X, Hu ZD, Chen XG (2004) Interaction of isofraxidin with human serum albumin. Bioorgan Med Chem 12:469–474. doi:10.1016/j.bmc.2003.10.030
39. Sreerama N, Woody RW (1993) A self-consistent method for the analysis of protein secondary structure from circular dichroism. Anal Biochem 209:32–44
40. Whitmore L, Wallace BA (2004) DICHROWEB, an online server for protein secondary structure analyses from circular dichroism spectroscopic data. Nucleic Acids Res 32:668–673. doi:10.1093/nar/gkh371
41. Cui FL, Fan J, Li JP, Hu ZD (2004) Interactions between 1-benzoyl-4-pchlorophen -yl thiosemicarbazide and serum albumin: investigation by fluorescence spectroscopy. Bioorgan Med Chem 12:151–157. doi:10.1016/j.bmc.2003.10.018
42. Zhang YZ, Zhou B, Liu YX, Zhou CX, Ding XL, Liu Y (2008) Fluorescence study on the interaction of bovine serum albumin with P-Aminoazobenzene. J Fluoresc 18:109–118. doi:10.1016/j.bmc.2003.10.018
43. Xiao Q, Huang S, Liu Y, Tian FF, Zhu JC (2009) Thermodynamics, conformation and active sites of the binding of Zn–Nd hetero-bimetallic Schiff base to bovine serum albumin. J Fluoresc 19:317–326. doi:10.1007/s10895-008-0418-y
44. Tian JN, Liu JQ, Hu ZD, Chen XG (2005) Interaction of wogonin with bovine serum albumin. Bioorgan Med Chem 13:4124–4129. doi:10.1016/j.bmc.2005.02.065